

## ARTICLE OPEN



# The ratio of brain to liver glucose activity and disease activity in multiple myeloma

Sarah Dingli<sup>1</sup>, Paul Rothweiler<sup>1</sup>, Moritz Binder<sup>1</sup> , Joselle Cook<sup>1</sup> , Morie A. Gertz<sup>2</sup>, Suzanne Hayman<sup>2</sup>, Prashant Kapoor<sup>1</sup> , Taxiarchis Kourelis<sup>1</sup> , Shaji K. Kumar<sup>1</sup> , Mustaqeem Siddiqui<sup>1</sup> , Rahma Warsame<sup>2</sup>, Yi Lin<sup>1</sup> , Arthur G. Erdman<sup>1</sup> and David Dingli<sup>1</sup> ✉

© The Author(s) 2025

Changes in metabolic activity in tumor cells is one of the hallmarks of cancer. Cancer cells exhibit the Warburg effect with high glucose consumption for their energy needs. This provides the basis for imaging using <sup>18</sup>F-2-deoxy-D-glucose for positron emission tomography to assess tumor burden and response to therapy. We postulated that metabolically active tumors may compete with the brain for glucose uptake and evaluated glucose uptake in the brain and liver in patients with multiple myeloma in various states of response and relapse. The ratio of brain to liver glucose activity (B2LR) mirrors disease activity in myeloma, predicts the presence of extramedullary disease and is also predictive of a short response to chimeric antigen receptor T cell therapy. Patients with a low B2LR also have an inferior survival compared to patients with persistently higher B2LR values. Our simple metabolic ratio has prognostic implications in myeloma and other tumors.

*Blood Cancer Journal* (2025)15:90; <https://doi.org/10.1038/s41408-025-01280-2>

## INTRODUCTION

Metabolic imaging in the form of <sup>18</sup>F-2-fluoro-2-deoxy-D-glucose positron emission tomography combined with computed tomography (<sup>18</sup>F-FDG PET/CT) is a critical tool in the accurate staging of tumors and to assess the response to therapy. In multiple myeloma, PET/CT is recommended for the evaluation of disease burden, to determine the presence of extramedullary disease (EMD) and to document metabolic response to therapy [1–5]. Current recommendations suggest that results from this modality have prognostic implications [6]. For example, a complete metabolic response after chimeric antigen receptor T cell (CAR-T) therapy is associated with a higher probability of a prolonged response [7]. Imaging reports typically highlight sites of disease, and their change in size and metabolic activity in the form of standardized uptake value (SUV) and provide a Deauville score from 1 to 5 to describe the state of the disease. The SUV is derived from the concentration of radioactivity in a given region of interest as a function of the injected dose of radioactivity per kilogram of body weight. An SUV greater than 2.5 is generally associated with a neoplastic process, although this is not specific [8]. Most tumors are very metabolically active and depend on glycolysis as their main source of adenosine triphosphate. This phenomenon is known as the Warburg effect and results in the increased uptake and retention of glucose by tumor cells [9]. Under normal physiologic conditions, most of the glucose in the circulation is used by the brain for its metabolism [10, 11]. Thus, the brain appears ‘hot’ in PET/CT imaging. We hypothesized that given the propensity of tumors to exhibit the Warburg effect, that tumors may compete with the brain for blood glucose uptake and that PET/CT image analysis of uptake in the

brain versus the liver would vary in patients with active disease versus those in remission. We chose the liver as the comparator since it is often considered to have a relatively constant glucose uptake. For our analysis, we initially focused on a cohort of patients with multiple myeloma cared for by the senior author at a center of excellence for this disease and where imaging was performed using a standard algorithm for reproducibility. Subsequently, we studied 134 patients with multiple myeloma who had PET/CT imaging performed immediately prior to chimeric antigen receptor T cell therapy (CAR-T).

## METHODS

After approval from the Institutional Review Board at Mayo Clinic, an initial cohort of 56 patients with multiple myeloma under the care of the senior author was identified. Demographic, clinical, and relevant laboratory characteristics were abstracted. All positron emission tomography combined with computerized tomography (PET/CT) using 18-fluorodeoxyglucose (<sup>18</sup>FDG) performed at Mayo Clinic in Rochester as part of the routine monitoring of these patients were identified and reviewed. PET/CT imaging was performed using standard protocols as approved by the Food and Drug Administration. Image analysis was performed using Qreads software. For each PET/CT image set, 5 regions of interest (ROI) from the cerebral cortex (vertex, frontal, right and left parietal, and occipital) were defined and the intensity of the radioactivity was determined using functionality in Qreads (Fig. 1). These regions were chosen because the cerebral cortex is the most metabolically active part of the brain since it is dense with neurons that consume 75% of the energy requirements of the brain [10, 11]. From the same set of scans, 5 ROI within the liver including both right and left lobes were also identified and <sup>18</sup>F pixel intensity determined.

<sup>1</sup>Earl E. Bakken Medical Devices Center, Department of Mechanical Engineering, College of Science and Engineering, University of Minnesota, Twin Cities, MN, USA. <sup>2</sup>Division of Hematology and Department of Internal Medicine, Mayo Clinic, Rochester, MN, USA. ✉email: dingli.david@mayo.edu

Received: 8 January 2025 Revised: 17 March 2025 Accepted: 2 April 2025

Published online: 07 May 2025

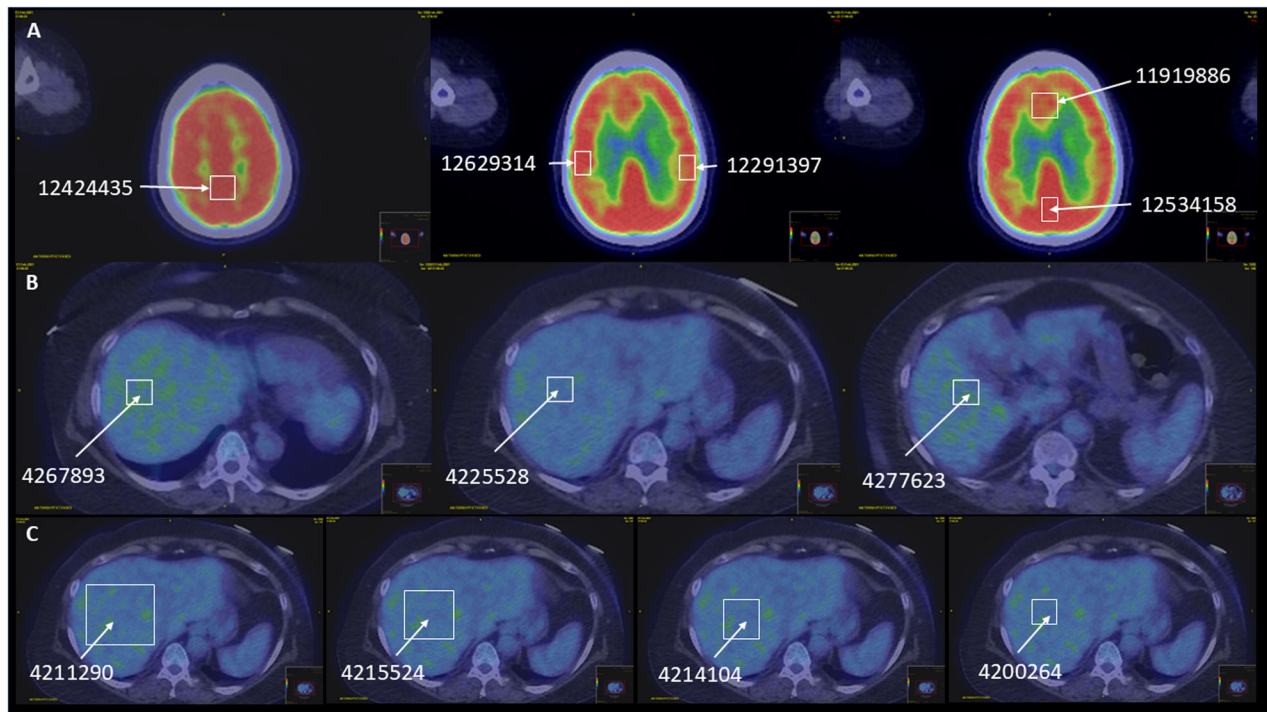


**Fig. 1 Region of interest analysis in the brain and liver.** We chose 5 areas in the brain to determine pixel intensity due to radioactive glucose uptake (A). Five ROIs were also chosen from the liver (B). The average activity in each ROI does not vary significantly as a function of the area of the ROI itself (C).

The average activity in the brain and in the liver was calculated and the brain to liver ratio (B2LR) determined for that image set. In total, 297 PET/CT image sets were analyzed in the first cohort of patients to test the hypothesis. Subsequently, we determined the B2LR in a cohort of 134 patients with myeloma who received commercial CAR-T at Mayo Clinic. All patients had PET/CT imaging performed between 7 and 10 days before the start of lymphoid depletion chemotherapy and all patients had to be off any plasma cell directed therapy (including steroids) for at least 2 weeks.

Cytogenetic risk assessment was based on the International Myeloma Working Group (IMWG) classification [12]. The patient's response to therapy was based on the IMWG definition of complete response (CR) [13]. Patients who relapsed after achieving CR were labeled as 'relapsed disease' and a response that was inferior to a CR but with no evidence of relapse or progression was labeled 'partial response'. We identified a subset of patients with EMD based on their imaging results and with histologic proof of extramedullary myeloma. This subset was chosen due to its independent prognostic significance and studied independently (see results).

To further test the validity of our approach, after IRB approval, we identified a cohort of 134 patients with multiple myeloma who had PET/CT before their CAR-T cell therapy. We determined their B2LR by reviewing each PET/CT (a total of 1340 ROI) and studied the impact of the B2LR on PFS and OS in this cohort.

Statistical analyses were performed using JMP Pro 17.0.0 (SAS Institute, Cary, NC, USA). Comparisons between means were with Student's *t* test and the Bonferroni correction was performed in the case of multiple comparisons. The Mann-Whitney test was used to compare between medians. Correlations were evaluated with Pearson's test. A  $p < 0.05$  was required for statistical significance. Overall survival (OS) was calculated from the date of diagnosis till death or last contact with the patient, with appropriate censoring. Comparisons between groups with respect to survival were performed using the Kaplan-Meier method with censoring. Progression free survival (PFS) was calculated from the time of an intervention until relapse or death whichever came first with appropriate censoring.

#### Ethics approval and consent to participate

All the methods used in this study were performed in accordance with the relevant guidelines and regulations. Approval from the Mayo Clinic

Institutional Review Board (IRB) was obtained to proceed with this study (IRB: 23-002940, 24-003662, 25-000198) and all patients had provided written informed consent for the use of their medical record including medical images to be included for this research.

#### RESULTS

We initially identified 56 patients with multiple myeloma, 33 were males and 23 females. The median age at diagnosis was 66.5 years (range: 40.3–82.7). Most were Caucasian (51/56) with two patients being African American and three Hispanic. Six patients had a concomitant diagnosis of diabetes mellitus. The median body mass index (the mass in kilogram divided by height in meters squared) was 28.6 (range: 20.4–45.2). The median number of PET/CT per patient was 4 (range: 1–24). High-risk cytogenetics were documented in 32 (57%) patients at some time point during the life history with the disease while 16 patients (28.6%) had evidence of EMD at some time during follow up of their multiple myeloma. Of the 16 patients with evidence of EMD based on imaging, histological confirmation of the diagnosis was confirmed in 13 of these patients. EMD was confirmed in the liver (3 patients), perinephric space (3 patients), soft tissues (4 patients), lymph nodes (3 patients) and pleural mass (1 patient). Some patients had evidence of EMD in more than one site and on multiple PET/CT imaging sets.

Initially, we wanted to determine the impact of the area of the ROI on the measurements of average pixel intensity. As can be seen from Fig. 1, the variability in pixel intensity between the largest and smallest ROI was 0.26% in the liver. Subsequently, we determined the intra-patient and inter-patient variability in pixel intensity in the brain and liver of patients in remission. We reasoned that the patients in remission would have the least variability and provide a useful baseline to evaluate the viability of our approach. There was very limited variability either in the brain or liver (Supplementary Fig. 1) across patients while in remission. We did not observe differences in the activity between the 5 ROI

**Table 1.** The brain to liver ratio (B2LR) across disease states in multiple myeloma.

State	Remission	Relapsed disease	Partial response	EMD
Mean	2.8894	2.5391	2.7406	2.5468
Median	2.8296	2.7802	2.7661	2.7209
Range	2.304–3.827	1.156–3.539	0.94–3.531	0.925–3.096
Standard Deviation	0.236723	0.805057	0.382062	0.624426

EMD extramedullary disease.

**Table 2.** Statistical comparison of the B2LR means and medians across the disease states in multiple myeloma.

State	Remission	Partial Response	Relapsed Disease	EMD
Remission		0.00932 <sup>b</sup>	0.575 <sup>b</sup>	0.00228 <sup>b</sup>
Partial Response	0.0059 <sup>a</sup>		0.01174 <sup>b</sup>	0.20054 <sup>b</sup>
Relapsed Disease	0.045 <sup>a</sup>	0.0286 <sup>a</sup>		0.00228 <sup>b</sup>
EMD	0.0016 <sup>a</sup>	0.1292 <sup>a</sup>	0.0048 <sup>a</sup>	

Pairwise comparisons between the various groups (with Bonferroni correction when applicable).

EMD extramedullary disease.

<sup>a</sup>represents comparisons between means.

<sup>b</sup>represents comparisons between medians.

chosen in the brain and liver for patients in remission, with relapsed disease, in a partial response or with EMD (Supplementary Figs. 2 and 3). Within an individual patient, the pixel intensity in the brain and liver and the calculated B2LR remained stable if the disease was in remission, at least over a 2-year interval (Supplementary Fig. 4). We found no correlation between the brain pixel intensity due to glucose uptake and age for the range of 40 to 82 years (Pearson's  $\rho = -0.09982$ ,  $p = 0.4684$ ) but liver uptake positively correlated with age ( $\rho = 0.3016$ ,  $p = 0.0252$ ). This led to an overall negative correlation of the B2LR with age ( $\rho = -0.2965$ ,  $p = 0.0279$ ). The BMI had an impact on the B2LR: a higher BMI was associated with less liver glucose uptake ( $\rho = -0.1694$ ,  $p = 0.2119$ ), higher uptake of radioactive glucose in the brain ( $\rho = 0.2377$ ,  $p = 0.0778$ ) and a positive correlation between the BMI and the B2LR ( $\rho = 0.2771$ ,  $p = 0.0387$ ). These results are likely compatible with the metabolic syndrome and insulin resistance that reduces hepatic glucose uptake, leading to higher blood glucose concentrations and perhaps higher glucose uptake in the brain. Normalization of the B2LR for the BMI at the time of the PET/CT resulted in an improvement in statistical significance when comparing the B2LR of patients in CR versus those with relapsed disease ( $p = 0.045$ ), with all the other comparisons remaining significant with  $p$  values of  $< 0.05$ .

We divided the imaging data into 4 cohorts: remission, partial response, relapsed disease and EMD and compared the median B2LR between the groups. These results are summarized in Table 1. The B2LR is highest in patients in remission (median: 2.8296) and lowest in patients with the presence of EMD (median 2.7209), while patients with partial response or relapsed disease had intermediate values (2.7661 and 2.7802, respectively). Pairwise comparisons of the B2LR between groups show that the differences are highly statistically significant (except for medians comparing patients in a remission compared to those with relapse of their disease (Table 2). Given that the patients with partial response and relapsed disease have radiologic evidence of disease activity, we pooled these two groups together as 'residual disease' and compared them with patients in remission or with EMD. The results are reported in Table 3. The difference with patients who have EMD remains and there is statistically significant difference between patients in remission and those with residual disease ( $p = 0.0337$ ).

**Table 3.** Statistical comparison of the B2LR across pooled data.

State	Remission	Residual disease	EMD
Remission		0.1031 <sup>b</sup>	0.00228 <sup>b</sup>
Residual Disease	0.0337 <sup>a</sup>		0.0164 <sup>b</sup>
EMD	0.0016 <sup>a</sup>	0.0203 <sup>a</sup>	

The means are in blue and medians in red.

EMD extramedullary disease.

<sup>a</sup>represents comparisons between means.

<sup>b</sup>represents comparisons between medians.

The B2LR changes in individual patients as a function of disease activity. In Fig. 2 we provide a representative example of a patient with serial PET/CT imaging data. In remission, the B2LR was 2.977 which decreased to 2.801 with relapse, improved again to 2.868 with a response and dropped to 2.631 with the second relapse. As can be seen from Figs. 3 and 4, evaluation of the activity in the brain can mirror the disease state in all possible scenarios (from response, to stable disease and relapse) with distinct changes in intracerebral glucose uptake that are often identifiable with a visual inspection alone but can be better quantified using the ROI analysis described of the pixel intensity due to  $^{18}\text{F}$ -FDG activity in the brain and liver for comparison. Serial measurements of activity in the brain and liver with the B2LR calculation matches the disease activity in patients as shown in Fig. 5 and Supplementary Fig. 5.

A comparison of the B2LR in remission versus residual disease across the patient population suggests that there is no specific B2LR threshold that is able to distinguish patients as being in remission or with any residual active disease (Table 2) or partial response across patients; the ratio appears to be dependent on the individual patient. However, when the B2LR is less than 2.5, the probability that the patient is in remission is only 3.6% at best, implying that most patients with a  $\text{B2LR} \leq 2.5$  have active disease. Moreover, our analysis suggests that  $\text{B2LR} \leq 2.5$  is associated with a high probability of EMD given that 13 of the 41 (31.7%) PET/CT images with evidence of this condition had such a B2LR value or lower. In contrast, only 8 out of 109 (7.3%) PET/CT with active disease ( $\chi^2 = 14.69$ ,  $p = 0.000126$ ) and 7 out of 91 (7.6%) with a



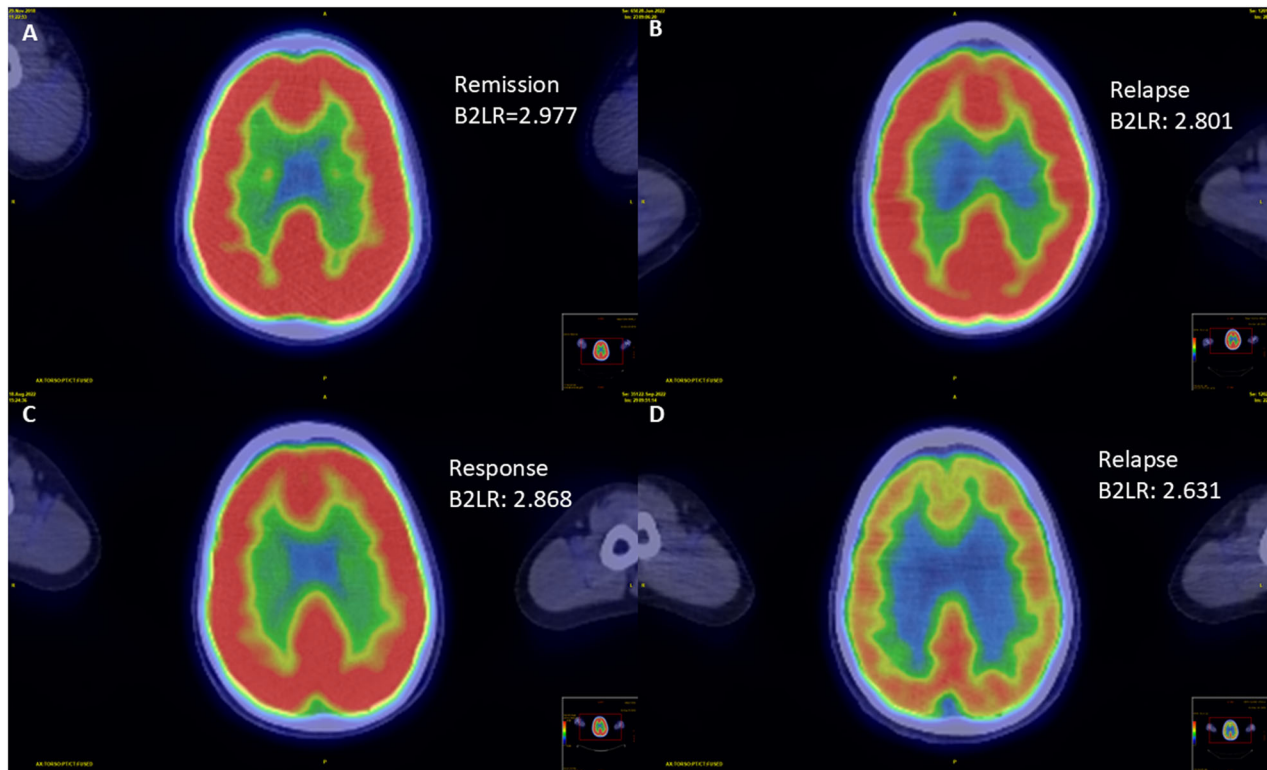


**Fig. 2 The B2LR correlates with disease activity.** Serial PET/CT imaging in the same patients at various time points in their disease showing how the pixel intensity due to radioactive glucose uptake and the B2LR change with the value being highest while in remission (A), the value decreases with relapse (B), increases again as the disease comes under control (C), and decreases further with the second relapse (D).

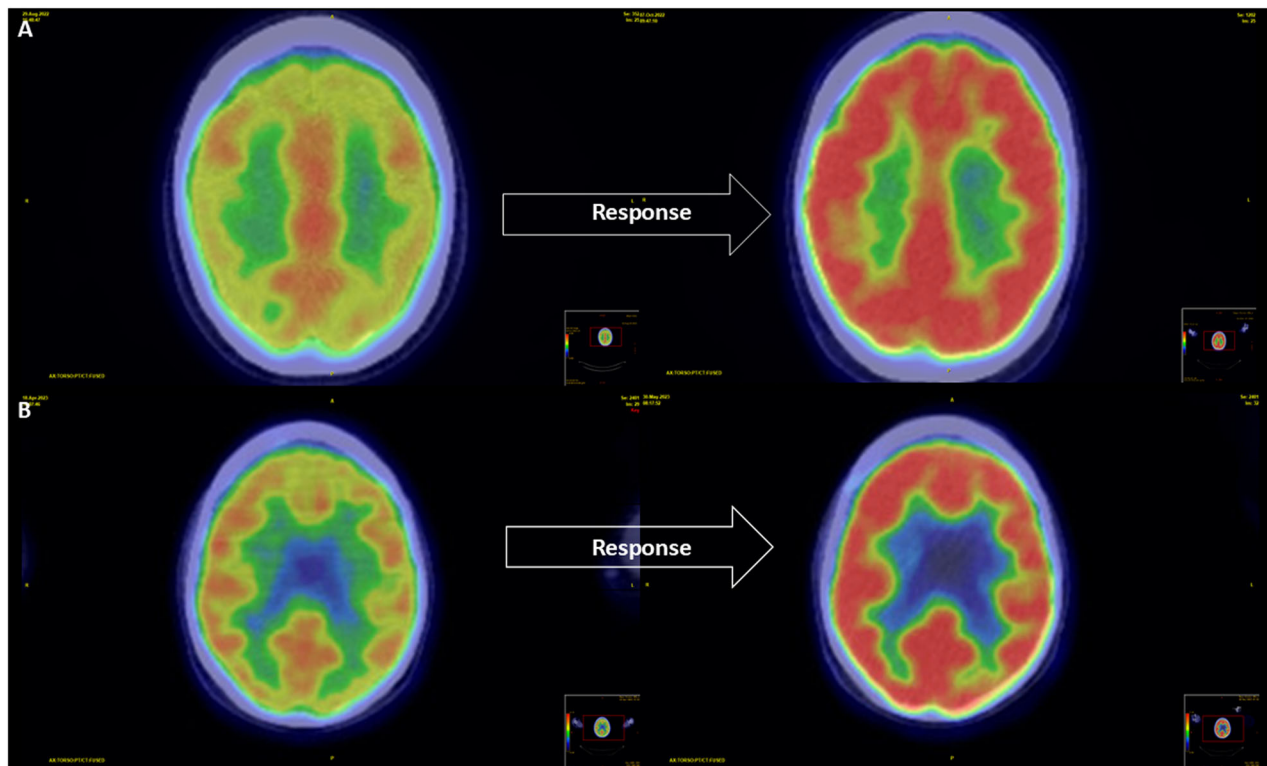


**Fig. 3 Generalizability of B2LR in response to changes in disease activity.** A, B provide examples from other patients where the brain uptake of glucose is low with active disease and improves with response to therapy.

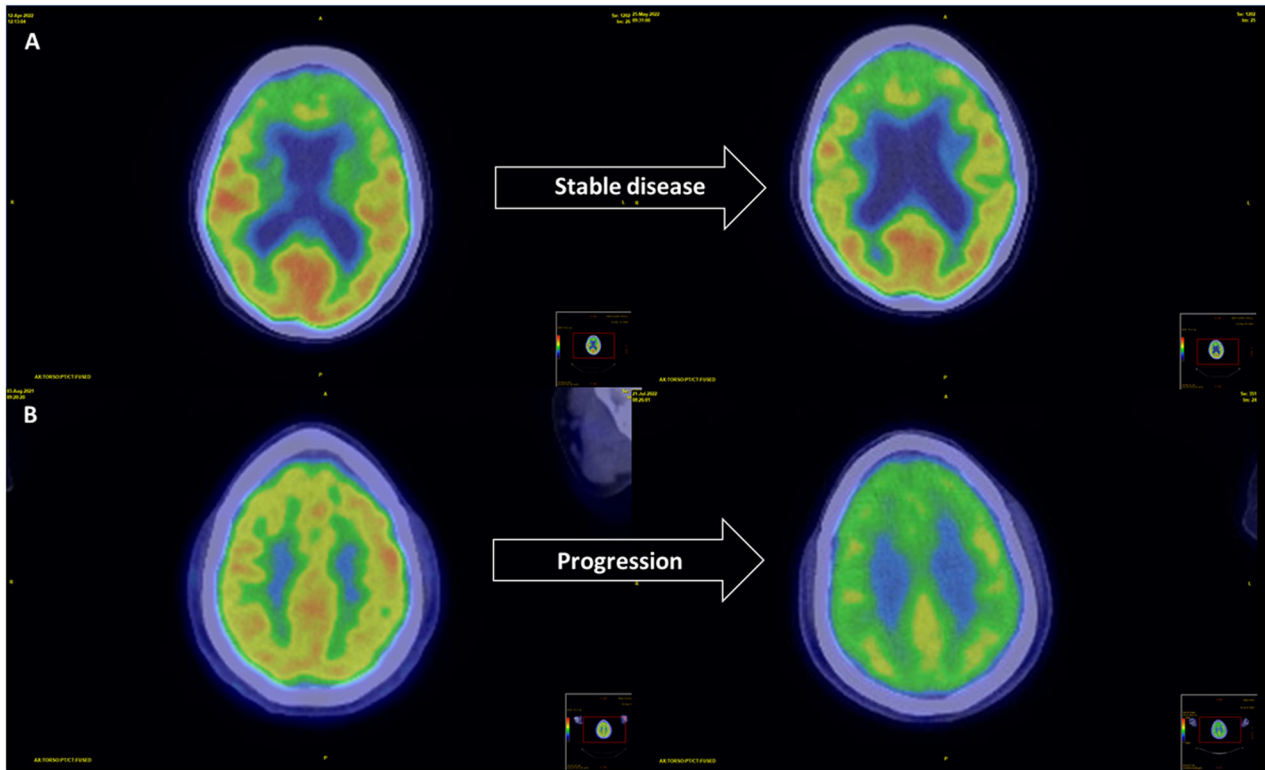


**Fig. 4 Disease stability and relapse.** Representative examples from additional patients showing stability of glucose uptake in a patient with stable disease in response to therapy (A) while in B decreased glucose uptake due to progressive disease is represented.

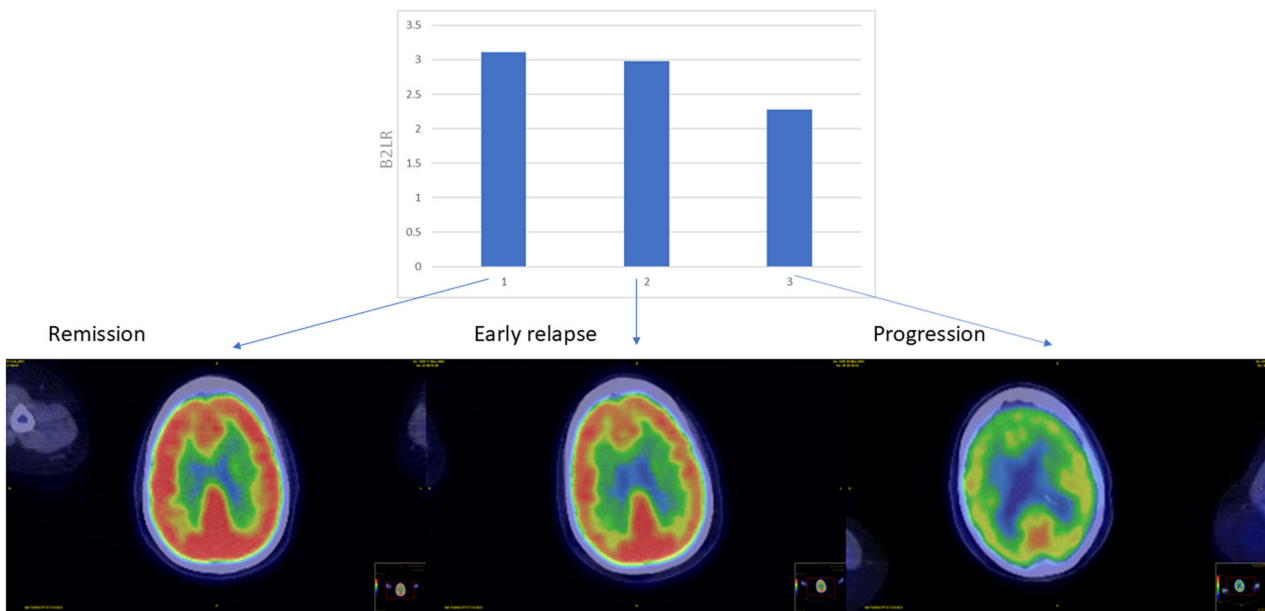


**Fig. 5 B2LR and relapsed disease.** A representative set of images from a patient with a high B2LR while in remission and serial reduction in the ratio with worsening disease progression.

partial response had such a low B2LR ( $\chi^2 = 12.6799$ ,  $p = 0.00037$ ). This threshold cannot distinguish between patients with partial response or active disease. The comparison between all 4 groups showed highly statistically significant differences and returned a  $\chi^2 = 25.2039$ ,  $p = 0.000014$ .

In Fig. 6, it also appears that patients with a  $B2LR \geq 3.0$  are unlikely to have evidence of EMD. Only 1 patient with radiologic evidence of EMD had such a high B2LR compared to patients in

remission ( $14/56$ ,  $\chi^2 = 9.2163$ ,  $p = 0.002399$ ) or patients with active disease ( $\chi^2 = 9.2563$ ,  $p = 0.002347$ ) or patients with a partial response ( $\chi^2 = 2.7049$ ,  $p = 0.10004$ ). This threshold can also imply a state of remission versus partial response ( $\chi^2 = 4.9816$ ,  $p = 0.02562$ ) since only 11% of patients in a partial response will have such a high B2LR compared to 25% of patients in remission. Finally, a comparison across the 4 groups gives a  $\chi^2 = 14.5366$ ,  $p = 0.002259$ . We also combined the patients with partial

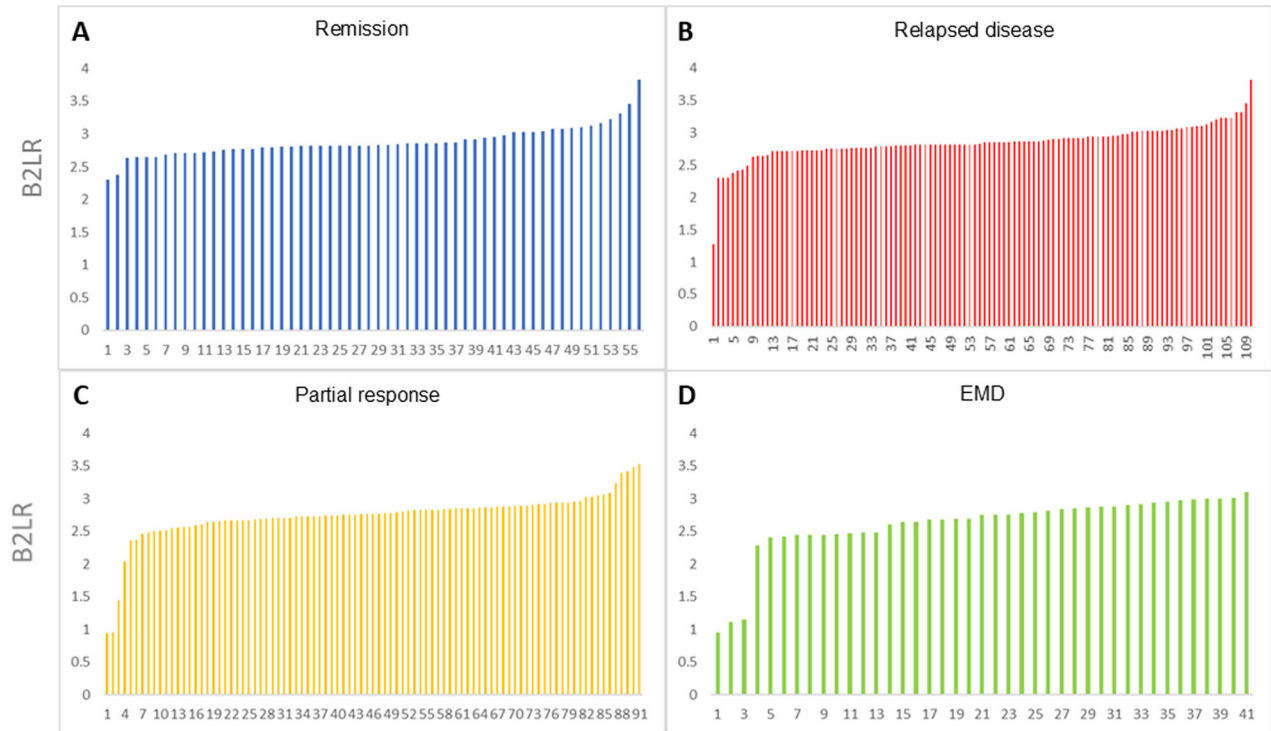


**Fig. 6 Distributions of the B2LR as a function of disease status.** The values of the B2LR for individual patients at each state of disease: **A** disease in remission, **B** relapsed disease, **C** partial response to therapy and **D** in the presence of EMD are plotted based on rank. The statistical comparisons between the groups are presented in Table 2.

response and relapsed disease using this  $B2LR \geq 3$  threshold. An analysis between the 3 groups (remission, residual disease and EMD), yields a  $\chi^2 = 8.7662$ ,  $p = 0.012487$ .

As an internal check on the data, we estimated the impact of high-risk cytogenetics on the outcome of patients with multiple myeloma. As expected, patients with no evidence of high-risk cytogenetics had a median survival of 3613 days, compared to a median of 2896 days for patients who had high-risk cytogenetics at any time point in their disease ( $p = 0.05$ ) (data not shown). Given the dichotomy in results with  $2.5 < B2LR < 3.0$  we sought to determine whether these thresholds have an impact on survival. The initial analysis was restricted to patients who underwent therapy with chimeric antigen receptor T cells (CAR-T). If the B2LR immediately before CAR-T therapy was  $\leq 2.5$ , the median duration of response was 231 days, compared to 328 days for patients whose  $B2LR > 2.5$  ( $p = 0.05$ ) (Supplementary Fig. 6A). Subsequently, we divided the patients into those who at any time had a  $B2LR \leq 2.5$  and those whose  $B2LR > 2.5$  at all-time points. We found that patients with a  $B2LR > 2.5$  at all-times had a median OS of 3480 days compared to 2896 days for patients who at any time had a  $B2LR \leq 2.5$  (Gehan Breslow  $p = 0.0375$ ) (Supplementary Fig. 6B). However, a  $B2LR > 3.0$  at any time point had no impact on OS: median OS for patients who at any time had a  $B2LR > 3.0$  was 3246 days compared to 3,301 days for patients who always had a  $B2LR < 3.0$  ( $p = 0.31$ ). Finally, we compared OS in patients who at any time had a  $B2LR \leq 2.5$  and  $B2LR > 3.0$  with all other patients who had B2LR between 2.5 and 3.0 at all-time points. Patients with  $2.5 \leq B2LR < 3.0$  had a median OS of 3480 days, while those patients who had  $B2LR \leq 2.5$  and  $B2LR > 3.0$  at any time in their disease course had a median OS of 2896 days ( $p = 0.12$ ).

Given the impact of the B2LR on this heterogeneous population of patients, we wanted to test its validity using a larger cohort of patients with multiple myeloma who were treated with commercial CAR-T at Mayo Clinic in Rochester. We included all patients treated between June 2021 and May 2024 to provide us with at

least 6-month of follow up. The demographic, clinical and laboratory characteristics of this cohort of patients is provided in Supplementary Table 1. Sixty-one patients received Ide-cel while 73 were treated with Cilta-cel. The two groups were well matched for gender and age at the time of treatment. More than 95% of patients were lenalidomide refractory and 77.1% of them had high-risk disease based on FISH. All patients had been treated with immunomodulatory agents, proteasome inhibitors and CD38 targeting monoclonal antibodies as required by the FDA label at the time of therapy. Bridging therapy was prescribed to 87% of patients and there was evidence of EMD in 23.3% of patients prior to CAR-T therapy. Twenty patients had a  $B2LR \leq 2.5$  prior to the start of lymphoid depletion chemotherapy. Patients treated with Ide-cel had a median of 5 (range: 3–13) prior lines of therapy, while patients treated with Cilta-cel had a median of 4 (range 3–9) prior lines of treatment ( $p = 0.019$ ). There was no difference in the serum LDH ( $p = 0.7478$ ), ferritin ( $p = 0.2746$ ) bone marrow plasma cell burden ( $p = 0.292$ ) and plasma cell labeling index ( $p = 0.9671$ ) between the two cohorts prior to CAR-T.

We determined the impact of various established parameters and the  $B2LR \leq 2.5$  on both PFS and OS in this cohort using the Cox proportional hazard method. On univariate analysis, the serum ferritin (HR:13.49,  $p = 0.0002$ ) [14, 15], the presence of EMD (HR:1.94,  $p = 0.0464$ ), bone marrow MRD negativity at 1-month (HR: 2.36,  $p = 0.0125$ ), MRD negativity at 3-months (HR: 3.96,  $p = 0.0123$ ) and  $B2LR \leq 2.5$  (HR:3.02,  $p = 0.0027$ ) were significant. On multivariate analysis for PFS, only the  $B2LR \leq 2.5$  (HR: 3.74,  $p = 0.0118$ ) and being MRD negative at 3-months (HR: 1.55,  $p = 0.0476$ ) retained significance. With respect to OS, on univariate analysis, the presence of EMD (HR: 2.38,  $p = 0.0333$ ),  $B2LR \leq 2.5$  (HR: 5.52,  $p < 0.0001$ ) and MRD negativity at 3-months (HR: 13.5,  $p = 0.0306$ ) were significant. On multivariate analysis only the  $B2LR \leq 2.5$  remained significant ( $p = 0.0234$ ) with respect to overall survival. In our analysis the use of neither Ide-cel nor Cilta-cel had an impact on PFS ( $p = 0.4942$ ) or OS ( $p = 0.4375$ ) in

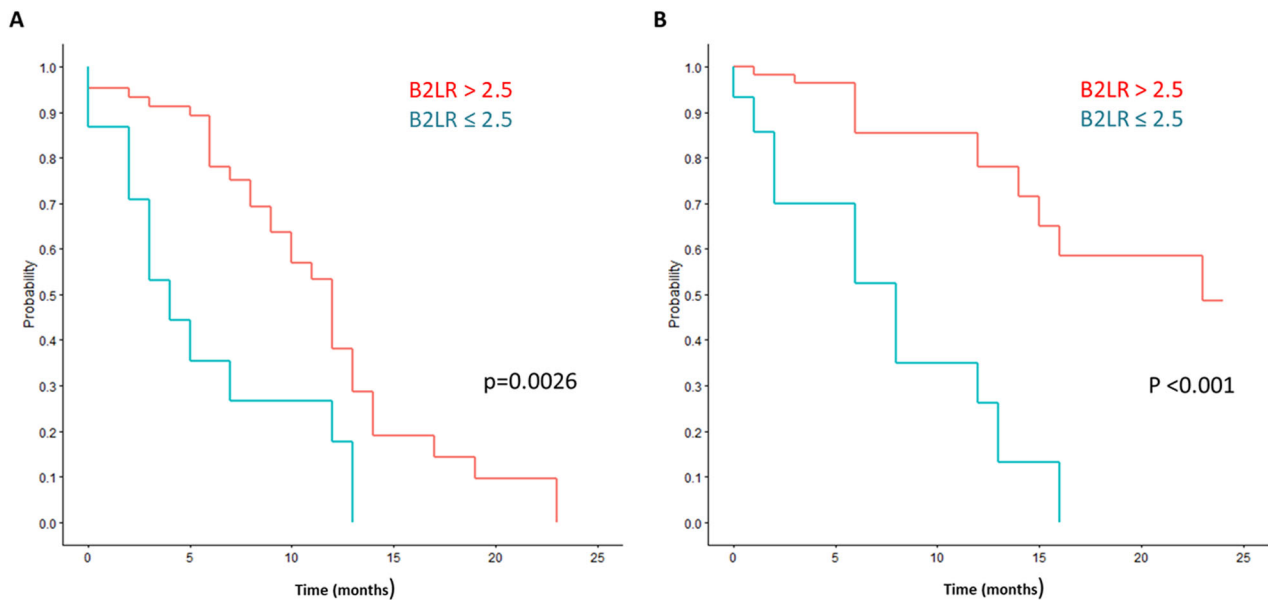


**Fig. 7** Survival analysis of 134 patients as a function of the B2LR before CAR-T therapy. In (A), the progression free survival as a function of the B2LR is presented. Patients with B2LR > 2.5 had a median PFS of 12 months compared to 4 months for patients with B2LR ≤ 2.5 ( $p = 0.0026$ ). In (B), overall survival for patients with B2LR > 2.5 was 23 months versus 8 months for those patients with B2LR ≤ 2.5 before CAR-T ( $p < 0.001$ ).

the univariate analysis. Patients with a B2LR > 2.5 had a median PFS of 12 months while those with B2LR ≤ 2.5 has a median PFS of 4 months (log-rank test,  $p = 0.0026$ ) (Fig. 7A). Similarly, patients with a B2LR > 2.5 had a median OS of 23 months compared to 8 months for patients with B2LR ≤ 2.5 (log-rank test,  $p < 0.001$ ) (Fig. 7B).

## DISCUSSION

The tumor burden is an important prognostic marker in multiple myeloma and risk stratification systems depend in part on this property of the tumor [12, 16]. However, other biological characteristics are also important including cytogenetics [12], the fraction of cells in 'S phase' [17], mutational landscape [18–20], presence of circulating plasma cells [21] and duration (or lack) of response to therapy have important prognostic implications in this disease. Tumor metabolic activity is also important, and in this respect, elevated serum lactate dehydrogenase levels are associated with a poor prognosis [22, 23]. Underlying  $^{18}\text{F}$ -FDG PET/CT imaging is the ability of tumor cells to transport and retain radioactive glucose for their metabolism. This is now considered an important characteristic of most tumors and part of the process of malignant transformation [9]. There are many approaches to use nuclear imaging to quantitate the tumor burden and determine its impact on outcomes [24]. Another approach that is being developed is in the theranostic space where specific imaging is used to infer potential therapeutic options. Determining the tumor burden based on imaging requires sophisticated software to analyze the images [24, 25]. In the current work, we show that the B2LR can provide very valuable information about disease activity with the B2LR increasing when the patient responds to therapy and decreasing if there is relapsed disease. The ratio is particularly low in patients with EMD. However, apart from its insights into disease activity, the index provides prognostic information about the state of multiple myeloma. Moreover, patients who have a B2LR ≤ 2.5 at any time in their history of multiple myeloma appear to have an inferior OS with a median of 2896 days compared to 3480 days for patients who never had a B2LR ≤ 2.5, a median difference of 584 days which is clinically very meaningful and also statistically significant.

Similarly, patients with a B2LR ≤ 2.5 immediately before proceeding to CAR-T therapy had a median duration of response of 231 days compared to 328 days for patients with a higher B2LR, a finding that was both clinically and statistically significant. It is interesting that patients with wide fluctuations in the B2LR had an inferior median OS of 2896 days compared to patients with narrower fluctuations in the B2LR (3480 days) perhaps suggesting that patients with highly metabolically active disease are more likely to progress and fail therapies. These results were confirmed by the larger analysis of 134 patients who received CAR-T therapy after a median of 4.5 lines of therapy. The B2LR remained the strongest predictor of both PFS and OS with patients having a B2LR ≤ 2.5 immediately before CAR-T having a particularly poor duration of response and a median overall survival of less than a year.

Our work has several limitations, including the relatively small size of the sample used to test the hypothesis, although this is not very different from other publications that evaluated the prognostic impact of PET/CT imaging in tumors [25, 26]. However, the validation data based on the 134 patients treated with commercial CAR-T provides further support for the hypothesis. While we cannot fully exclude the potential of a skewed population due to the referral practice where the patients were evaluated, the sample size makes this concern less likely. One of the strengths of the study is that all patients were evaluated and treated at a single center and imaged using the same algorithms and with complete data to characterize the features of their disease. We do not make any claim that the B2LR correlates with tumor burden as measured by other approaches such as metabolic tumor volume or total lesion glycolysis, but simply that it correlates with disease activity and appears prognostic.

What is intriguing is the independent predictive power of the B2LR in patients being considered for therapy with CAR-T. In our analysis of 134 patients, the B2LR emerged as the single most important predictor of both PFS and OS, even independent of the presence of EMD. Indeed, while on univariate analysis EMD was a predictor of both PFS and OS, this parameter lost its significance in the multivariate model. In our analysis, lenalidomide refractoriness as well as the presence of high-risk FISH abnormalities lost their prognostic significance, likely due to the high frequency of these



abnormalities in our cohort of patients treated with CAR-T. Similarly, the serum ferritin also lost its significance and as we reported elsewhere [27], a serum ferritin cut-off of  $>400 \mu\text{g/L}$  had no impact on survival [14, 15]. Our observations suggest that the B2LR could be considered for decision making prior to CAR-T cell therapy given the potential toxicity of the treatment and the short duration of response in those with a B2LR  $<2.5$ . Perhaps we should pause before proceeding with CAR-T in patients with such a low ratio given the complex logistics of the therapy and the inevitable anguish related to a short response. At present we do not know whether the same ratio could be informative with respect to the duration of response to other multiple myeloma therapies such as stem cell transplant or bispecific antibodies and this will require further study. The potential role of the ratio in risk stratification of smoldering or newly diagnosed multiple myeloma will also need to be explored.

It is possible that these findings may apply to other types of tumors, since the underlying pathobiology is shared by virtually all cancers and given the ubiquity of PET/CT imaging in all fields of oncology. Indeed, the fundamental principle is the reprogramming of cellular energy metabolism leading to glycolysis as the main provider of cellular energy, a phenomenon that is considered an emerging hallmark of cancer [9]. In conclusion, the B2LR based on PET/CT imaging in multiple myeloma provides insights into the activity of the disease as well as prognostic information with respect to overall survival and progression free survival after chimeric antigen receptor T cell therapy.

## DATA AVAILABILITY

The datasets generated and/or analysed during the current study are available from the corresponding author on reasonable request.

## REFERENCES

- Bailly C, Carlier T, Jamet B, Touzeau C, Moreau P, Kraeber-Bodere F, et al. (18)F-FDG PET/CT in multiple myeloma: critical insights and future directions. *Eur J Nucl Med Mol Imaging*. 2019;46:1048–50. <https://doi.org/10.1007/s00259-019-04279-7>.
- Rajkumar SV, Dimopoulos MA, Palumbo A, Blade J, Merlini G, Mateos MV, et al. International myeloma working group updated criteria for the diagnosis of multiple myeloma. *Lancet Oncol*. 2014;15:e538–48. [https://doi.org/10.1016/S1470-2045\(14\)70442-5](https://doi.org/10.1016/S1470-2045(14)70442-5).
- Cavo M, Terpos E, Nanni C, Moreau P, Lentzsch S, Zweegman S, et al. Role of (18)F-FDG PET/CT in the diagnosis and management of multiple myeloma and other plasma cell disorders: a consensus statement by the International Myeloma Working Group. *Lancet Oncol*. 2017;18:e206–17. [https://doi.org/10.1016/S1470-2045\(17\)30189-4](https://doi.org/10.1016/S1470-2045(17)30189-4).
- Hillengass J, Usmani S, Rajkumar SV, Durie BGM, Mateos MV, Lonial S, et al. International myeloma working group consensus recommendations on imaging in monoclonal plasma cell disorders. *Lancet Oncol*. 2019;20:e302–12. [https://doi.org/10.1016/S1470-2045\(19\)30309-2](https://doi.org/10.1016/S1470-2045(19)30309-2).
- Charalampous C, Goel U, Broski SM, Dingli D, Kapoor P, Gertz MA, et al. Utility of PET/CT in assessing early treatment response in patients with newly diagnosed multiple myeloma. *Blood Adv*. 2022;6:2763–72. <https://doi.org/10.1182/bloodadvances.2022007052>.
- Nanni C, Zamagni E. Fluorodeoxyglucose-PET/computed tomography as a predictor of prognosis in multiple myeloma. *PET Clin*. 2019;14:383–9. <https://doi.org/10.1016/j.cpet.2019.03.005>.
- Costa LJ, Usmani SZ. Defining and managing high-risk multiple myeloma: current concepts. *J Natl Compr Canc Netw*. 2020;18:1730–7. <https://doi.org/10.6004/jncn.2020.7673>.
- Im HJ, Bradshaw T, Solaiyappan M, Cho SY. Current methods to define metabolic tumor volume in positron emission tomography: which one is better? *Nucl Med Mol Imaging*. 2018;52:5–15. <https://doi.org/10.1007/s13139-017-0493-6>.
- Hanahan D, Weinberg RA. Hallmarks of cancer: the next generation. *Cell*. 2011;144:646–74. <https://doi.org/10.1016/j.cell.2011.02.013>.
- Mergenthaler P, Muselmann C, Sunwoldt J, Isaev NK, Wieloch T, Dirnagl U, et al. A functional role of the cyclin-dependent kinase inhibitor 1 (p21(WAF1/CIP1)) for neuronal preconditioning. *J Cereb Blood Flow Metab*. 2013;33:351–5. <https://doi.org/10.1038/jcbfm.2012.213>.
- Magistretti PJ, Allaman I. A cellular perspective on brain energy metabolism and functional imaging. *Neuron*. 2015;86:883–901. <https://doi.org/10.1016/j.neuron.2015.03.035>.
- Chng WJ, Dispenzieri A, Chim CS, Fonseca R, Goldschmidt H, Lentzsch S, et al. IMWG consensus on risk stratification in multiple myeloma. *Leukemia*. 2014;28:269–77. <https://doi.org/10.1038/leu.2013.247>.
- Kumar S, Paiva B, Anderson KC, Durie B, Landgren O, Moreau P, et al. International Myeloma Working Group consensus criteria for response and minimal residual disease assessment in multiple myeloma. *Lancet Oncol*. 2016;17:e328–e46. [https://doi.org/10.1016/S1470-2045\(16\)30206-6](https://doi.org/10.1016/S1470-2045(16)30206-6).
- Gagelmann N, Dima D, Merz M, Hashmi H, Ahmed N, Tovar N, et al. Development and validation of a prediction model of outcome after B-cell maturation antigen-directed chimeric antigen receptor T-cell therapy in relapsed/refractory multiple myeloma. *J Clin Oncol*. 2024;42:1665–75. <https://doi.org/10.1200/JCO.23.02232>.
- Sidana S, Patel KK, Peres LC, Bansal R, Kocoglu MH, Shune L, et al. Safety and efficacy of standard of care ciltacabtagene autoleucel for relapsed/refractory multiple myeloma. *Blood*. 2024. Epub 20241004. <https://doi.org/10.1182/blood.2024025945>.
- Greipp PR, San Miguel J, Durie BG, Crowley JJ, Barlogie B, Blade J, et al. International staging system for multiple myeloma. *J Clin Oncol*. 2005;23:3412–20. <https://doi.org/10.1200/JCO.2005.04.242>.
- Greipp PR, Lust JA, O'Fallon WM, Katzmann JA, Witzig TE, Kyle RA. Plasma cell labeling index and beta 2-microglobulin predict survival independent of thymidine kinase and C-reactive protein in multiple myeloma. *Blood*. 1993;81:3382–7.
- Walker BA, Wardell CP, Murison A, Boyle EM, Begum DB, Dahir NM, et al. APOBEC family mutational signatures are associated with poor prognosis translocations in multiple myeloma. *Nat Commun*. 2015;6:6997. <https://doi.org/10.1038/ncomms7997>.
- Bolli N, Biancon G, Moarii M, Gimondi S, Li Y, de Philippis C, et al. Analysis of the genomic landscape of multiple myeloma highlights novel prognostic markers and disease subgroups. *Leukemia*. 2018;32:2604–16. <https://doi.org/10.1038/s41375-018-0037-9>.
- Bolli N, Genuardi E, Ziccheddu B, Martello M, Oliva S, Terragna C. Next-generation sequencing for clinical management of multiple myeloma: ready for prime time? *Front Oncol*. 2020;10:189. <https://doi.org/10.3389/fonc.2020.00189>.
- Gonsalves WL, Jevremovic D, Nandakumar B, Dispenzieri A, Buadi FK, Dingli D, et al. Enhancing the R-ISS classification of newly diagnosed multiple myeloma by quantifying circulating clonal plasma cells. *Am J Hematol*. 2020;95:310–5. <https://doi.org/10.1002/ajh.25709>.
- Gkotzamanidou M, Kastritis E, Gavriatopoulou MR, Nikitas N, Gika D, Mparmparousi D, et al. Increased serum lactate dehydrogenase should be included among the variables that define very-high-risk multiple myeloma. *Clin Lymphoma Myeloma Leuk*. 2011;11:409–13. <https://doi.org/10.1016/j.clml.2011.07.001>.
- Palumbo A, Avet-Loiseau H, Oliva S, Lokhorst HM, Goldschmidt H, Rosinol L, et al. Revised international staging system for multiple myeloma: a report from international myeloma working group. *J Clin Oncol*. 2015;33:2863–9. <https://doi.org/10.1200/JCO.2015.61.2267>.
- Marchiori S, Cousin F, Papadopoulos I, Bernard C, Thys M, De Prijck B, et al. Prognostic value of visual IMPeTUs criteria and metabolic tumor burden at baseline [(18)F]FDG PET/CT in patients with newly diagnosed multiple myeloma. *EJNMMI Res*. 2024;14:51. <https://doi.org/10.1186/s13550-024-01113-6>.
- Breen WG, Young JR, Hathcock MA, Kowalchuk RO, Thorpe MP, Bansal R, et al. Metabolic PET/CT analysis of aggressive Non-Hodgkin lymphoma prior to Axicabtagene Ciloleucel CAR-T infusion: predictors of progressive disease, survival, and toxicity. *Blood Cancer J*. 2023;13:127. <https://doi.org/10.1038/s41408-023-00895-7>.
- Dean EA, Haskar RS, Lu H, Mousa MS, Krivenko GS, Lazaryan A, et al. High metabolic tumor volume is associated with decreased efficacy of axicabtagene ciloleucel in large B-cell lymphoma. *Blood Adv*. 2020;4:3268–76. <https://doi.org/10.1182/bloodadvances.2020001900>.
- Dingli S, Rothweiler P, Blander M, Cook J, Gertz MA, Hayman S, et al. Implications of lymphocyte kinetics after chimeric antigen receptor T cell therapy for multiple myeloma. *Leukemia*. 2025; <https://doi.org/10.1038/s41375-025-02547-0>.

## ACKNOWLEDGEMENTS

Funding for this project was provided by The Centurion Fund through the Department of Development at Mayo Clinic, in support of DD. Input from Dr Brad J. Kemp from the Department of Radiology, Mayo Clinic is greatly appreciated.

## AUTHOR CONTRIBUTIONS

Concept: SD, PR, AGE, and DD. Data abstraction and analysis: SD and DD, manuscript preparation: SD and DD. Critical review and final manuscript approval: SD, PR, AGE, and DD. Patient care, critical review of manuscript, final approval of manuscript: MB, JC, MAG, SH, PK, TK, SKK, MS, RW, YL, and DD.



## COMPETING INTERESTS

SD, PR, MB, JC, SH, MS, RW, and AGE have no disclosures. MAG: Personal fees from Ionis/Akcea, honorarium from Alnylym, personal fees from Prothena, personal fees from Sanofi, personal fees from Janssen, personal fees for Data Safety Monitoring board from Abbvie & Arcellex, fees from Johnson & Johnson, Honoraria from Astra Zeneca, Medscape, Dava Oncology. Alexion and NCI SPORE MM SPORE 5P50 CA186781-04. PK: Clinical trial support with research funding to the institution from Amgen, Regeneron, Bristol Myers Squibb, Loxo Pharmaceuticals, Ichnos, Karyopharm, Sanofi, AbbVie and GlaxoSmithKline. Honorarium from Keosys and served on the Advisory Boards of BeiGene, Mustang Bio, Janssen, Pharmacyclics, X4 Pharmaceuticals, Kite, Oncoceptides, Ascentage, Angitia Bio, GlaxoSmithKline, Sanofi and AbbVie. TK: Research funding to institution: Pfizer. SKK: Consulting with no personal payment: AbbVie, Amgen, ArcellX, Beigene, BMS, Carsgen, GSK, Janssen, K36, Moderna, Pfizer, Regeneron, Roche-Genentech, Sanofi, Takeda, (with personal payments): CVS Caremark, BD Biosciences. Clinical trial support to institution - AbbVie, Amgen, Astra Zeneca, BMS, Carsgen, GSK, Gracell Bio, Janssen, Oricell, Roche-Genentech, Sanofi, Takeda, Telogenomics. YL: Ad Boards: Janssen, Sanofi, BMS, Regeneron, Genentech, Tessera, Legend, NexT Therapeutics. Steering Committees: Janssen, Kite/Gilead. Research: Janssen, BMS. Scientific Advisory Boards: NexImmune, Caribou. Data Safety Monitoring Board: Pfizer. DD: Consulting with personal payment: Alexion, Apellis, Argenyx, BMS, Janssen, Regeneron, Roche-Genentech, Sanofi, Sorrento and Takeda. Clinical trial support to institution: K36 Therapeutics.

## ADDITIONAL INFORMATION

**Supplementary information** The online version contains supplementary material available at <https://doi.org/10.1038/s41408-025-01280-2>.

**Correspondence** and requests for materials should be addressed to David Dingli.

**Reprints and permission information** is available at <http://www.nature.com/reprints>

**Publisher's note** Springer Nature remains neutral with regard to jurisdictional claims in published maps and institutional affiliations.



**Open Access** This article is licensed under a Creative Commons Attribution-NonCommercial-NoDerivatives 4.0 International License, which permits any non-commercial use, sharing, distribution and reproduction in any medium or format, as long as you give appropriate credit to the original author(s) and the source, provide a link to the Creative Commons licence, and indicate if you modified the licensed material. You do not have permission under this licence to share adapted material derived from this article or parts of it. The images or other third party material in this article are included in the article's Creative Commons licence, unless indicated otherwise in a credit line to the material. If material is not included in the article's Creative Commons licence and your intended use is not permitted by statutory regulation or exceeds the permitted use, you will need to obtain permission directly from the copyright holder. To view a copy of this licence, visit <http://creativecommons.org/licenses/by-nc-nd/4.0/>.

© The Author(s) 2025